A theoretical study on the ionization of NO_2 with analysis of vibrational structure of the photoelectron spectrum

Kouichi Takeshita[a)]
Faculty of Bioindustry, Tokyo University of Agriculture, Abashiri, Hokkaido 099-24, Japan

Norihiro Shida
Department of Chemistry, Nagoya Institute of Technology, Gokiso-cho, Showa-ku, Nagoya, 466, Japan

(Received 2 April 2001; accepted 3 December 2001)

Ab initio calculations have been performed to study the molecular structures and the vibrational levels of the low-lying ionic states ($^1A_1$, $^3B_2$, $^3A_2$, $^1A_2$, $^1B_2$, $^1B_1$, $2\,^1A_1$, $^3B_1$, and $^3A_1$) of nitrogen dioxide. The global regions of the potential energy surfaces have been obtained by multireference single and double excitation configuration interaction calculations. Vibrational calculations using vibrational Hamiltonians have been used for vibrational analysis. The equilibrium molecular structures and a vibrational analysis of these states are presented. The theoretical ionization intensity curves including the vibrational structures of the ionic states are also presented and are compared with the photoelectron spectra. A new assignment of the photoelectron spectra has been proposed. © *2002 American Institute of Physics.* [DOI: 10.1063/1.1445742]

I. INTRODUCTION

The ground state of nitrogen dioxide is the $^2A_1$ state, whose electronic configuration is represented by $\ldots(5a_1)^2(1b_1)^2(4b_2)^2(1a_2)^2(6a_1)^1$ with the C_{2v} symmetry group.

He(I) photoelectron spectroscopy investigations of NO_2 have been published by various authors.[1–3] Brundle *et al.*[2] have reported the seven bands below 19 eV. The first broad-band was assigned to the $^1A_1(6a_1)^{-1}$ state. The second, third, fourth, and fifth bands between 12.5 and 15 eV were assigned to the $^3B_2(4b_2)^{-1}$, $^3A_2(1a_2)^{-1}$, $^1A_2(1a_2)^{-1}$, and $^1B_2(4b_2)^{-1}$ states, respectively, which show resolved vibrational structure. The vibrational structure of the second, third, and fifth bands were assigned to the ν_2 bending mode and that of the fourth band to the ν_1 stretching and ν_2 bending modes. The sixth and seventh band between 17 and 18.8 eV have a long vibrational progression. They have suggested that the $^3A_1(5a_1)^{-1}$ and $^3B_1(1b_1)^{-1}$ states contributed to those bands. The vibrational progression was assigned to the ν_1 stretching mode.

Theoretical studies of the photoelectron spectrum have been reported.[4,5] Kimura *et al.*[4] have obtained the vertical ionization energies by the configuration interaction method. Their assignment of band below 15 eV was consistent with that by Brundle *et al.* However, the bands of 17–18.8 eV were assigned to $^1B_1$, $^3B_1$, and $^3A_1$ states. The vertical ionization energy of the $2\,^1A_1$ state was reported, which was assigned to the band above 18.8 eV.

As far as we are aware, there is neither a theoretical study of the molecular structures with a vibrational analysis of the ionic states, nor a theoretical study on the vibrational structures of photoelectron spectra. In this paper, we theoretically examine the molecular structures and the vibrational structure of the photoelectron spectra.

We have undertaken vibrational analysis using the vibrational Hamiltonians, which have the global region of the potential energy surface calculated at the multireference single and double excitation configuration interaction (MRSDCI) level, and the exact G matrix. Using these calculations, we obtained vibrational wave functions, Franck–Condon factors (FCFs), and intensity curves. The vibrational structure of the photoelectron spectrum is discussed by using the calculated quantities.

II. METHOD OF CALCULATIONS

We used the split valence type basis sets of the MIDI-4-type prepared by Tatewaki and Huzinaga.[6] These were augmented by one *d*-type polarization function for N and O. The exponents of the polarization function for N and O are 0.87 and 1.16, respectively.

The multireference single and double excitation configuration interaction (MRSDCI) method was used to get the global regions of the potential energy surfaces. The molecular orbitals for the MRSDCI calculations of the ionic states except for the $^1A_1$ state were obtained by the open shell Roothaan's restricted Hartree–Fock method. In the MRSDCI calculations, singly and doubly excited configuration state functions (CSFs) were generated from reference CSFs, while N_{1s} and O_{1s} orbitals were kept frozen. The number of reference CSFs of the $^2A_1$, $^1A_1$, $^3B_2$, $^3A_2$, $^1A_2$, $^1B_2$, $^1B_1$, $2\,^1A_1$, $^3B_1$, and $^3A_1$ states are 2, 3, 3, 3, 3, 3, 4, 6, 3, and 3, respectively.

We calculated the global regions of the potential energy surfaces, where the equilibrium molecular structures of both the ground and the ionic states are included. The intervals of the bond length and the bond angle were 0.02 Å and 10°, respectively.

a)Electronic mail: take@ec.hokudai.ac.jp

 © 2002 American Institute of Physics

Using the above-mentioned scheme of calculation, the electronic energies at about 200 different geometry points were calculated to construct the potential energy surfaces for each state. The form of the vibrational Hamiltonian used in this work is

$$\hat{H}(r_1,r_2)=\frac{1}{2}(\hat{P}_{r_1}\hat{P}_{r_2})\begin{pmatrix} G_{r_1r_1}(r_1,r_2) & G_{r_1r_2}(r_1,r_2) \\ G_{r_2r_1}(r_1,r_2) & G_{r_2r_2}(r_1,r_2)\end{pmatrix} \times\begin{pmatrix}\hat{P}_{r_1}\\ \hat{P}_{r_2}\end{pmatrix}+V(r_1,r_2), \quad (1)$$

where $V(r_1,r_2)$ is the energy surface and $G(r_1,r_2)$ is the so-called Wilson's G matrix defined as follows:

$$G_{r_ir_j}=\sum_{k}^{3N}\frac{\partial r_i}{\partial X_k}\frac{\partial r_j}{\partial X_k} \quad (X_k\text{: mass-weighted Cartesian coordinate}). \quad (2)$$

The coordinates r_1 and r_2 were defined as a bond length N–O and a bond angle O–N–O, respectively. The analytical expressions of $V(r_1,r_2)$ were obtained by the least-squares fitting using eight order polynomial functions. The G matrices were evaluated by Eq. (2) using the molecular geometries where the potential energies were calculated. These discrete values of the G matrices were also fitted to six order polynomial functions. (Note that the changing of the G matrices with respect to the internal coordinates is explicitly included in the calculations.) The eigenstates of the vibrational Hamiltonian were obtained by the basis set expansion method. The forms of the basis set expansions we used are as follows:

$$\Psi(r_1,r_2)=\sum_{i}^{m}\sum_{j}^{n}C_{ij}f_i(r_1)g_j(r_2), \quad (3a)$$

$$f_i(r_1)=(r_1-r_{10i})^{S_i}\exp(-\alpha_i(r_1-r_{10i})^2), \quad (3b)$$

$$g_j(r_2)=(r_2-r_{20j})^{t_j}\exp(-\beta_j(r_2-r_{20j})^2). \quad (3c)$$

The eigenstates were solved by optimizing the variational parameters, C, α, and β. Typically, the numbers of m and n in Eq. (3) were 30 and 30. The numerical errors of the vibrational energies within the above-given scheme of calculation are thought to be at most a few wave numbers. The Franck–Condon factors were calculated directly from the overlap integrals of the wave functions of Eq. (3a) in the ground and the excited states. The method of calculation of the FCFs and theoretical intensity curves were the same as used in our previous paper.[7]

This work was carried out by using the ALCKEMY II[8–10] program for the MRSDCI calculations. The VIBR4[11] program was used for vibrational analysis calculations involving considering the global region of the potential energy surface.

III. RESULTS AND DISCUSSION

The optimized geometrical parameters of the ground and nine ionic states ($^1A_1$, $^3B_2$, $^3A_2$, $^1A_2$, $^1B_2$, $^1B_1$, $2\,^1A_1$, $^3B_1$, and $^3A_1$) are listed in Table I, which also shows a magnitude of the change in the bond length and bond angle upon ionization. The molecular structure of the $^1A_1$ state is linear, while those of the other states are bend. For the $^1A_1$ and $^1B_1$ states, the magnitude of the changes in both the bond length and bond angle are larger than that of the other state. For the $^3B_1$ and $^3A_1$ states, the magnitude of the change in the bond length is about +0.1 Å.

TABLE I. Optimized structure and magnitude of the change upon ionization. The values in parentheses are the magnitude of the change in geometry upon ionization. The experimental values (Ref. 12) of R_{N-O} and O–N–O of $^2A_1$ are 1.193 Å and 134.1°, respectively.

State	R_{N-O} (Å)	(ΔR_{N-O}) (deg)	O–N–O(ΔO–N–O) (Å)	(deg)
$^2A_1$	1.185		135	
$^1A_1$	1.120	(−0.065)	180	(+45)
$^3B_2$	1.199	(+0.014)	122	(−13)
$^3A_2$	1.209	(+0.024)	130	(−5)
$^1A_2$	1.209	(+0.024)	131	(−4)
$^1B_2$	1.205	(+0.020)	125	(−10)
$^1B_1$	1.271	(+0.086)	98	(−37)
$2\,^1A_1$	1.236	(+0.051)	108	(−27)
$^3B_1$	1.284	(+0.099)	131	(−4)
$^3A_1$	1.280	(+0.095)	134	(−1)

The 0–0 ionization energies (I.E.s) and the Franck–Condon factors (FCFs) of the 0–0 transitions are given in Table II. For the $^3A_2$ and $^1A_2$ states, the FCFs of the 0–0 transition are beyond 0.5. Therefore, the 0–0 transitions of these states have maximum intensity in their vibrational levels. For the $^1A_1$, $2\,^1A_1$, and $^1B_1$ states, an observation of the 0–0 transition should be impossible because of the negligibly small value of the FCF.

The reference functions and the weight of the reference function of the MRSDCI calculations at the optimized geometry are shown in Table III. The main configurations of the $^1A_1$, $^3B_2$, $^3A_2$, $^1A_2$, and $^1B_2$, states correspond to the single electron ionization of $(6a_1)^{-1}$, $(4b_2)^{-1}$, $(1a_2)^{-1}$, $(1a_2)^{-1}$, and $(4b_2)^{-1}$ from the main configuration of the ground state, respectively. For these states, the weight of the main configuration is about 80%. The main configuration of the $^1B_1$ state is $\ldots(6a_1)^2(1b_1)^2(4b_2)^1(1a_2)^1$, which corresponds to the double electron excitations of $(4b_2)^{-1}(1a_2)^{-1}$. The weight of the main configuration is 80%, while the weight of the CSF corresponding to the single electron ionization of $(1b_1)^{-1}$ is 3%. For the $2\,^1A_1$ state, the main configuration is $\ldots(5a_1)^2(6a_1)^2(1b_1)^2(1a_2)^2$, which corresponds to the double electron ex-

TABLE II. The 0–0 transitional state.

State	I.E. (eV)	Expt. (eV)[a]	FCF
$^1A_1$	8.73	⋯	0.000
$^3B_2$	12.05	12.85	0.068
$^3A_2$	12.70	13.60	0.608
$^1A_2$	13.10	14.07	0.666
$^1B_2$	13.81	14.37	0.254
$^1B_1$	15.16		0.000
$2\,^1A_1$	15.66		0.000
$^3B_1$	16.57	16.99, 17.06	0.010
$^3A_1$	16.60		0.024

[a]The experimental values are from Brundle *et al.* (Ref. 2).

TABLE III. The reference functions of the MRSDCI calculation.

State	Reference function	Weight(%)
$^2A_1$[a]	$...(6a_1)^1(1b_1)^2(4b_2)^2(1a_2)^2$	86.8
	$...(6a_1)^1(1b_1)^2(2b_1)^2(4b_2)^2$	1.8
$^1A_1$	$...(1b_1)^2(4b_2)^2(1a_2)^2$	85.3
	$...(6a_1)^1(1b_1)^2(2b_1)^1(4b_2)^1(1a_2)^1$	2.4
	$...(1b_1)^2(1a_2)^2(6a_1)^2$	1.2
$^3B_2$	$...(6a_1)^1(1b_1)^2(4b_2)^1(1a_2)^2$	84.3
	$...(5a_1)^1(6a_1)^2(1b_1)^2(4b_2)^1(1a_2)^2$	2.3
	$...(5a_1)^1(6a_1)^1(1b_1)^2(2b_1)^1(4b_2)^2(1a_2)^1$	1.5
$^3A_2$	$...(6a_1)^1(1b_1)^2(4b_2)^2(1a_2)^1$	82.4
	$...(6a_1)^1(1b_1)^1(2b_1)^1(4b_2)^2(1a_2)^1$	5.2
	$...(6a_1)^1(2b_1)^2(4b_2)^2(1a_2)^1$	1.5
$^1A_2$	$...(6a_1)^1(1b_1)^2(4b_2)^2(1a_2)^1$	82.9
	$...(6a_1)^1(1b_1)^1(2b_1)^1(4b_2)^2(1a_2)^1$	4.2
	$...(6a_1)^1(2b_1)^2(4b_2)^2(1a_2)^1$	1.4
$^1B_2$	$...(6a_1)^1(1b_1)^2(4b_2)^1(1a_2)^2$	76.2
	$...(5a_1)^1(6a_1)^1(1b_1)^2(2b_1)^1(4b_2)^2(1a_2)^1$	6.1
	$...(1b_1)^2(2b_1)^1(4b_2)^2(1a_2)^1$	5.0
$^1B_1$	$...(6a_1)^2(1b_1)^2(4b_2)^1(1a_2)^1$	80.2
	$...(6a_1)^1(1b_1)^1(4b_2)^2(1a_2)^2$	3.0
	$...(6a_1)^2(1b_1)^1(2b_1)^1(4b_2)^1(1a_2)^1$	3.4
	$...(5a_1)^1(6a_1)^2(1b_1)^1(4b_2)^2(1a_2)^2$	1.4
$2\,^1A_1$	$...(5a_1)^2(6a_1)^2(1b_1)^2(1a_2)^2$	47.8
	$...(5a_1)^2(1b_1)^2(4b_2)^2(1a_2)^2$	16.4
	$...(5a_1)^2(6a_1)^1(1b_1)^2(2b_1)^1(4b_2)^1(1a_2)^1$	8.0
	$...(5a_1)^1(6a_1)^1(1b_1)^2(4b_2)^2(1a_2)^2$	4.4
	$...(6a_1)^2(1b_1)^2(4b_2)^2(1a_2)^2$	4.3
	$...(5a_1)^2(6a_1)^2(1b_1)^2(3b_2)^1(4b_2)^1(1a_2)^2$	3.5
$^3B_1$	$...(6a_1)^1(1b_1)^1(4b_2)^2(1a_2)^2$	55.8
	$...(6a_1)^1(1b_1)^2(2b_1)^1(4b_2)^2$	26.3
	$...(6a_1)^1(1b_1)^1(2b_1)^2(4b_2)^2$	4.9
$^3A_1$	$...(5a_1)^1(6a_1)^1(1b_1)^2(4b_2)^2(1a_2)^2$	59.1
	$...(5a_1)^2(6a_1)^1(1b_1)^2(2b_1)^1(4b_2)^1(1a_2)^1$	22.6
	$...(5a_1)^1(6a_1)^1(1b_1)^1(2b_1)^1(4b_2)^2(1a_2)^2$	2.4

[a]Total energy of $^2A_1$ is $-204.303\,147$ a.u.

citations of $(4b_2)^{-2}$. The weight of the main configuration is 48%. The CSFs of $...(5a_1)^2(1b_1)^2(4b_2)^2(1a_2)^2$ and $...(5a_1)^1(6a_1)^1(1b_1)^2(4b_2)^2(1a_2)^2$ correspond to the single electron ionization of $(6a_1)^{-1}$ and $(5a_1)^{-1}$, respectively. The weight of these CSFs are 16 and 4%. The main configurations of the $^1B_1$ and $2\,^1A_1$ states correspond to the single electron ionization of $(1b_1)^{-1}$ and $(5a_1)^{-1}$, respectively. The weight of these CSFs are 56% and 59%.

The vibrational frequencies of the totally symmetric vibrational modes of the ground and ionic states are listed in Table IV. The ν_1 and ν_2 modes are characterized as the N–O stretching and O–N–O bending modes, respectively.

Figure 1 illustrates the vibrational structure of the theoretical intensity curve (TIC) of the first ionic state ($^1A_1$) with a half width of 0.02 eV compared with the observed photoelectron spectrum (PES). The theoretical intensity curve shows a well-resolved vibrational structure, while the observed photoelectron spectrum shows a more complicated vibrational structure. The theoretical intensity curve shows the two vibrational progressions: progressions A and B. Vibrational levels over one hundred states (FCF>0.001) contribute to the vibrational progressions. An assignment of the vibrational progressions is given in Table V, where the vibrational levels of which FCF is beyond 0.01 are listed. The vibrational progression A consists of the three vibrational progressions of the ($2\,n$, $n=13-19$), ($4\,n$, $n=10-18$), and ($6\,n$, $n=11-14$) transitions. The vibrational progression B consists of the transitions of the ($3\,n$, $n=11-19$) and ($5\,n$, $n=10-16$) levels. The vibrational excitation for the higher energy levels of the ν_1 (N–O stretching) and ν_2 (O–N–O bending) modes contributes to the intensity. This is con-

TABLE IV. Vibrational frequency of the totally symmetric stretching mode (cm^{-1}).

State	ν_1(N–O)	ν_2(O–N–O)
$^2A_1$[a]	1500	793
$^1A_1$	1504	704
$^3B_2$	1480	678
$^3A_2$	1385	721
$^1A_2$	1393	713
$^1B_2$	1466	647
$^1B_1$	1416	659
$2\,^1A_1$	1752	995
$^3B_1$	1240	626
$^3A_1$	1202	628

[a]The observed values (Ref. 12) of the ν_1 and ν_2 modes of the $^2A_1$ state are 1320 and 750 cm^{-1}, respectively.

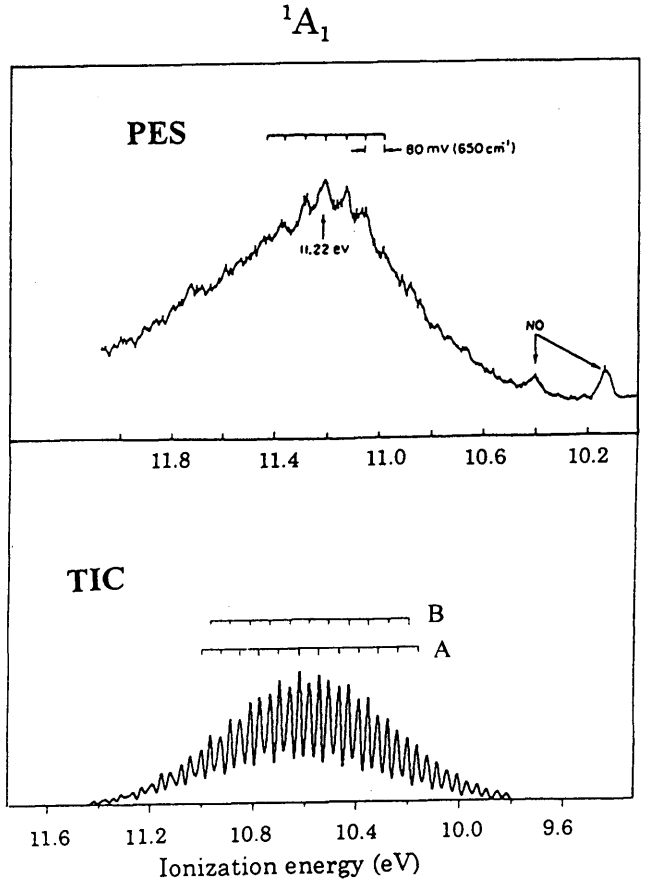

FIG. 1. The theoretical intensity curve of the $^1A_1$ state with a half width of 0.02 eV and the PE spectrum from Brundle *et al.* (Ref. 2). TIC: theoretical intensity curve and PES: photoelectron spectrum of the $^1A_1$ state.

TABLE V. Interpretation of the vibrational levels of the theoretical intensity curve of the $^1A_1$ state. The vibrational levels of FCF>0.01 are listed.

	Progression			
I.E.	A		B	
10.17	(2 13)			
10.20			(3 11)	
10.24	(2 14)			
10.28			(3 12)	
10.31–10.32	(2 15),	(4 10)		
10.36			(3 13)	
10.39–10.40	(2 16),	(4 11),		
10.43			(3 14)	
10.47	(2 17),	(4 12),		
10.50–10.51			(3 15),	(5 10)
10.54–10.55	(2 18),	(4 13)		
10.58–10.59			(3 16),	(5 11)
10.62–10.63	(2 19),	(4 14)		
10.65–10.67			(3 17),	(5 12)
10.70		(4 15)		
10.73–10.74			(3 18),	(5 13)
10.76–10.78		(4 16),	(6 11)	
10.81–10.82			(3 19),	(5 14)
10.84–10.86		(4 17),	(6 12)	
10.89				(5 15)
10.92–10.93		(4 18),	(6 13)	
10.97				(5 16)
11.00			(6 14)	

nected to the large magnitude of the changes in the bond length and the bond angle upon ionization. The bond angle becomes wide by 45°. The bond length becomes short by 0.073 Å. The vibrational spacing found in the progressions A and B is ascribed to the ν_2 mode. Brundle *et al.* have reported that the vibrational spacing found in the PES was 650 cm^{-1}, which was assigned to the ν_2 mode. The calculated value of the ν_2 frequency is 704 cm^{-1}. The theoretical intensity curve does not reproduce well the photoelectron spectrum (see Fig. 1). The vibrational spacing of progressions A or B of the TIC however agrees with that of the PES. The relative position between progressions A and B should not be good because of an error in calculation of the ν_1 and ν_2 frequencies.

The vibrational structure of the second ionic state ($^3B_2$) is shown in Fig. 2. The vibrational structure of the TIC with a half width of 0.02 eV reproduces well that of the PES. An interpretation of the vibrational peaks is given in Table VI. The vibrational progression of the (0 n, n=0–7) transitions has strong intensity. The progressions of the (1 n, n=0–6) and (2 n, n=1–4) transitions overlap to the above-mentioned progression. In all progressions, the excitation of the ν_2 O–N–O bending mode contributes to the intensity. The calculated values of the ν_1 and ν_2 frequencies are 1480 and 678 cm^{-1}, respectively. The observed value of ν_2 is 650 cm^{-1}.

The vibrational structure of the third and fourth ionic states ($^3A_2$ and $^1A_2$) is illustrated in Fig. 3. The vibrational structure of the TIC with a half width of 0.02 eV reproduces that of the PES. An interpretation of the vibrational peaks of the TIC of the $^3A_2$ state is found in Table VII. The vibrational structure of the $^3A_2$ state is interpreted as the (n 0, n

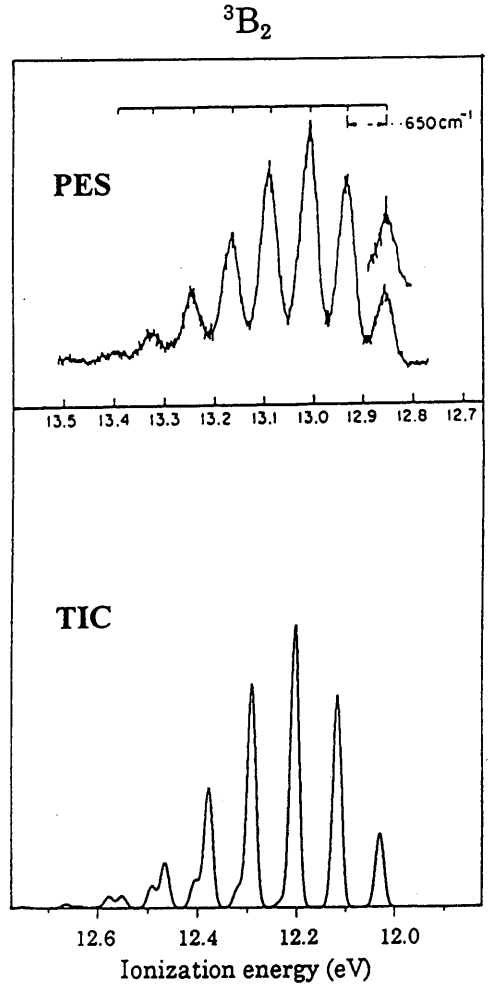

FIG. 2. The theoretical intensity curve of the $^3B_2$ states with a half width of 0.02 eV and the PE spectrum from Brundle *et al.* (Ref. 2).

=0–3) and (n 1, n=0–2) transitions. The vibrational progression of the 0–0 transition has strong intensity. The third peak was assigned to the (0 2) transition by Brundle *et al.* The present calculation suggests that the third peak should be assigned to the (1 0) transition. The calculated values of the ν_1 and ν_2 frequencies are 1385 and 721 cm^{-1}, respectively. The observed value of ν_2 is 650 cm^{-1}. An interpretation of the vibrational peaks of the TIC of the $^1A_2$ state is given Table VIII. The vibrational structure of the $^1A_2$ state is inter-

TABLE VI. Interpretation of the vibrational levels of the theoretical intensity curve of the $^3B_2$ state. Intensity is classified into S, M, or W according to the magnitude of FCF as follows: S: 0.25>FCF>0.1, M: 0.1>FCF >0.01, or W: 0.01>FCF>0.001.

I.E.	Progression		
12.04	M(0 0)		
12.13	S(0 1)		
12.21–12.23	S(0 2),	W(1 0)	
12.30–12.31	S(0 3),	M(1 1)	
12.38–12.39	S(0 4),	M(1 2)	
12.46–12.48	M(0 5),	M(1 3),	W(2 1)
12.55–12.56	M(0 6),	M(1 4),	W(2 2)
12.63–12.64	W(0 7),	W(1 5),	W(2 3)
12.73–12.74		W(1 6),	W(2 4)

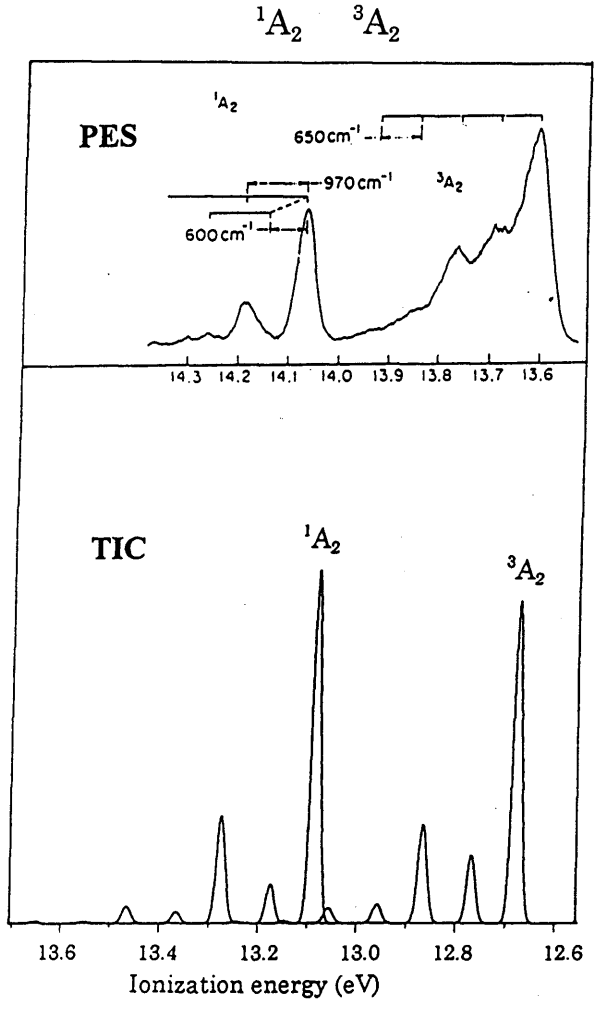

FIG. 3. The theoretical intensity curve of the $^3A_2$ and $^1A_2$ states with a half width of 0.02 eV and the PE spectrum from Brundle *et al.* (Ref. 2).

preted as the (n 0, n=0–3), (n 1, n=0–2) and (n 2, n =0–2) transitions. The vibrational progression of the (n 0, n=0–3) transitions has strong intensity and that of the (n 1, n=0–2) and (n 2, n=0–2) transitions has weak intensity. The calculated values of the ν_1 and ν_2 frequencies are 1393 and 713 cm^{-1}, respectively. The observed values of ν_1 and ν_2 are 970 and 600 cm^{-1}, respectively.

The vibrational structure of the fifth ionic state ($^1B_2$) is shown in Fig. 4. The vibrational structure of the TIC with a half width of 0.02 eV reproduces that of the PES. Table IX

TABLE VII. Interpretation of the vibrational levels of the theoretical intensity curve of the $^3A_2$ state. Intensity is classified into S, M, or W according to the magnitude of FCF as follows: S: 0.25>FCF>0.1, M: 0.1>FCF >0.01, or W: 0.01>FCF>0.001.

I.E.	Progression	
12.68	S(0 0)	
12.77		S(0 1)
12.86	S(1 0)	
12.94		M(1 1)
13.03	M(2 0)	
13.11		W(2 1)
13.19	W(3 0)	

TABLE VIII. Interpretation of the vibrational levels of the theoretical intensity curve of the $^1A_2$ state. Intensity is classified into S, M, or W according to the magnitude of FCF as follows: S: 0.25>FCF>0.1, M: 0.1>FCF >0.01, or W: 0.01>FCF>0.001.

I.E.	Progression		
13.09	S(0 0)		
13.18		M(0 1)	
13.26–13.27	S(1 0),		W(0 2)
13.35		M(1 1),	W(0 3)
13.43–13.44	M(2 0),		W(1 2)
13.52		W(2 1)	
13.60–13.61	W(3 0),		W(2 2)

gives an interpretation of the vibrational peaks. The vibrational structure is assigned to the (0 n, n=0–4), (1 n, n =0–4), (2 n, n=0–3), and (3 n, n=0–2) transitions. The vibrational progression of the (0 n, n=0–4) transitions has strong intensity at the lower energy sides of the spectrum. The calculated values of the ν_1 and ν_2 frequencies are 1466 and 647 cm^{-1}, respectively. The observed value of ν_2 is 620 cm^{-1}.

Table II indicates that the $^1B_1$, $2\,^1A_1$, $^3B_1$, and $^3A_1$ states should contribute to the photoelectron spectrum in the

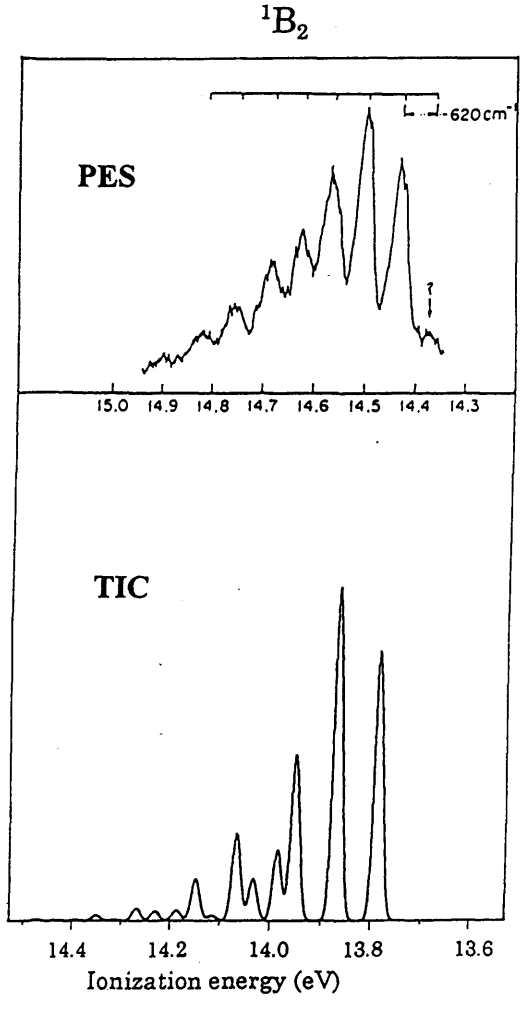

FIG. 4. The theoretical intensity curve of the $^1B_2$ state with a half width of 0.02 eV and the PE spectrum from Brundle *et al.* (Ref. 2).

TABLE IX. Interpretation of the vibrational levels of the theoretical intensity curve of the $^1B_2$ state. Intensity is classified into S, M, or W according to the magnitude of FCF as follows: S: 0.25>FCF>0.1, M: 0.1>FCF >0.01, or W: 0.01>FCF>0.001.

I.E.	Progression			
13.79	S(0 0)			
13.88	S(0 1)			
13.96–13.98	S(0 2),	M(1 0)		
14.04–14.06	M(0 3),	S(1 1)		
14.12–14.16	W(0 4),	M(1 2),	M(2 0)	
14.22–14.24		M(1 3),	M(2 1)	
14.29–14.31		W(1 4),	W(2 2),	W(3 0)
14.39–14.41			W(2 3),	W(3 1)
14.49				W(3 2)

16.8–18.2 eV energy range. A vibrational structure of the TIC with a half width of 0.02 eV of the $^1B_1$, $2\,^1A_1$, $^3B_1$, and $^3A_1$ is shown in Fig. 5, where the $^1B_1$ state shows a complicated vibrational structure, while the other states show a simple one.

The number of vibrational levels more than one hundred levels of FCF>0.001 contributes to the vibrational structure of the $^1B_1$ state. An interpretation of the vibrational structure is given in Table X, where the vibrational transitions of FCF >0.01 are listed. The higher vibrational excitations such as

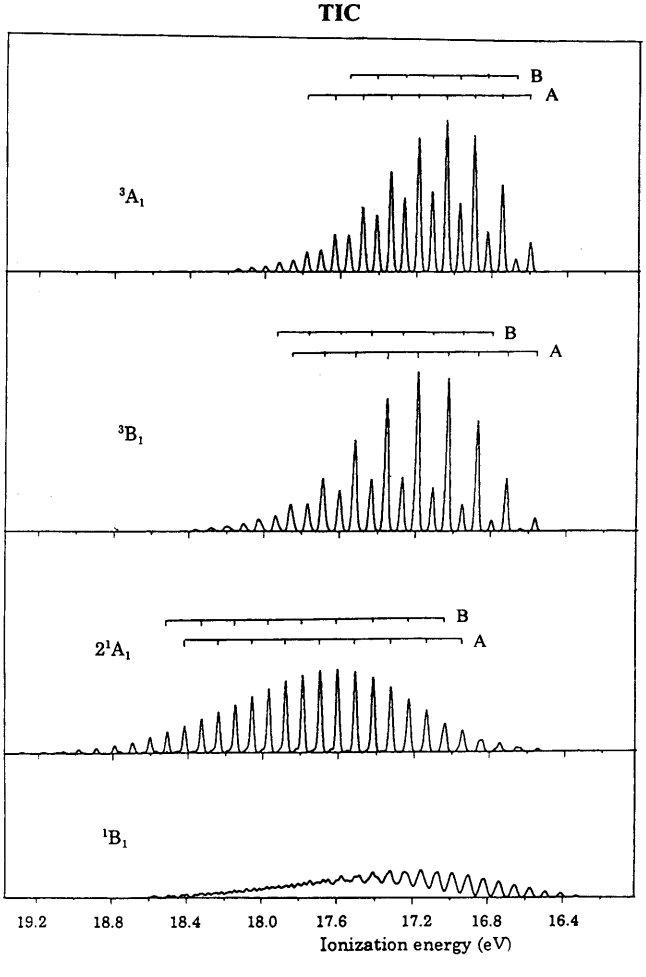

FIG. 5. The theoretical intensity curve of the $^1B_1$, $^3A_1$, $2\,^1A_1$, and $^3B_1$ state with a half width of 0.02 eV.

TABLE X. Interpretation of the vibrational levels of the theoretical intensity curve of the $^1B_1$ state. The vibrational levels of FCF>0.01 are listed.

I.E.	Progression		
17.06	(2 19)		
17.14–17.15	(2 20),	(3 18)	
17.22–17.24	(2 21),	(3 19)	
17.31–17.32	(2 22),	(3 20)	
17.39–17.41	(2 23),	(3 21)	
17.48–17.49	(2 24),	(3 22),	(4 20)
17.57		(3 23)	
17.64	(2 26)		

the (2 n, n=19–26) and (3 n, n=18–23) transitions contribute to the intensity. This situation is connected to the fact that the magnitude of the changes in both the bond length and the bond angle upon ionization are large (see Table I).

Figure 5 shows that the $2\,^1A_1$ state has the two vibrational progressions A and B. An interpretation of these vibrational progressions is found in Table XI. Progression A is assigned to the (n 0, n=7–14) and (n 2, n=5–7) transitions. Progression B is assigned mainly to the (n 1, n =6–14) transitions.

The $^3B_1$ state has the two vibrational progressions A and B. An interpretation of these vibrational progressions is given in Table XII. Progression A is assigned to the (n 0, n =0–8), (n 2, n=1–6), and (n 4, n=0–2) transitions. Progression B is assigned to the (n 1, n=3–7) and (n 3, n =1–4) transitions. Progression A has strong intensity. This is ascribed mainly to the (n 0, n=1–7) transitions.

The $^3A_1$ state has the two vibrational progressions A and B. Table XIII gives an interpretation of the vibrational progressions. Progression A is assigned to the (n 0, n=0–8) and (n 2, n=3–5) transitions. Progression B is assigned to

TABLE XI. Interpretation of the vibrational levels of the theoretical intensity curve of the $2\,^1A_1$ state. Intensity is classified into S, M, or W according to the magnitude of FCF as follows: S: 0.11>FCF>0.06, M: 0.06>FCF >0.03, or W: 0.03>FCF>0.01.

	Progression		
I.E.	A	B	
16.94	W(5 2)		
17.03–17.04		W(6 1),	W(5 3)
17.13–17.14	W(7 0), W(6 2)		
17.23		M(7 1)	
17.32–17.33	M(8 0), W(7 2)		
17.42		S(8 1)	
17.51	S(9 0)		
17.60		S(9 1)	
17.70	S(10 0)		
17.79		S(10 1)	
17.88	S(11 0)		
17.97		S(11 1)	
18.06	M(12 0)		
18.15		M(12 1)	
18.24	M(13 0)		
18.33		W(13 1)	
18.42	W(14 0)		
18.51		W(14 1)	

TABLE XII. Interpretation of the vibrational levels of the theoretical intensity curve of the $^3B_1$ state. Intensity is classified into S, M, or W according to the magnitude of FCF as follows: S: 0.11>FCF>0.06, M: 0.06>FCF >0.03, or W: 0.03>FCF>0.01.

	Progression				
I.E.	A		B		
16.57	W(0 0)				
16.72	M(1 0)				
16.87–16.88	S(2 0),	W(1 2),	W(0 4)		
16.95					W(1 3)
17.03–17.04	S(3 0),	M(2 2),	W(1 4)		
17.11				W(3 1)	W(2 3)
17.19–17.20	S(4 0),	W(3 2),	W(2 4)		
17.27–17.28				W(4 1),	W(3 3)
17.35–17.36	S(5 0),	W(4 2)			
17.43–17.44				M(5 1),	W(4 3)
17.52–17.53	S(6 0),	W(5 2),			
17.61				W(6 1)	
17.68–17.69	M(7 0),	W(6 2),			
17.77				W(7 1)	
17.86	W(8 0)				
17.94				W(8 1)	

the (n 1, n=0–6) and (n 3, n=2–5) transitions. Progression A has strong intensity. This is ascribed to the (n 0, n=1–6) transitions.

In both the $^3B_1$, and $^3A_1$ states, the higher vibrational excitations of the N–O stretching (ν_1) mode contribute to the intensity. This is connected to the large magnitude of the changes in the N–O bond length upon ionization (see Table I).

The overall feature of the vibrational structure for these four ionic states is illustrated in Fig. 6, where the ratio of transition moments of the $^1B_1$, $2\,^1A_1$, $^3B_1$, and $^3A_1$ states are estimated and found to be 0.22, 0.80, 0.97, and 1.0, respectively, from Table III. These values are estimated using the coefficient of the CSF, which corresponds to the single

TABLE XIII. Interpretation of the vibrational levels of the theoretical intensity curve of the $^3A_1$ state. Intensity is classified into S, M, or W according to the magnitude of FCF as follows: S: 0.11>FCF>0.06, M: 0.06>FCF >0.03, or W: 0.03>FCF>0.01.

	Progression			
I.E.	A		B	
16.60	W(0 0)			
16.67			W(0 1)	
16.74	S(1 0)			
16.82			M(1 1)	
16.89	S(2 0)			
16.97			M(2 1)	
17.04	S(3 0)			
17.11–17.12			W(3 1),	M(2 3)
17.19	S(4 0),	W(3 2)		
17.26–17.27			W(4 1),	M(3 3)
17.33–17.34	M(5 0),	M(4 2)		
17.41			W(5 1),	W(4 3)
17.48	M(6 0),	W(5 2)		
17.56			W(6 1),	W(5 3)
17.63	W(7 0)			
17.78	W(8 0)			

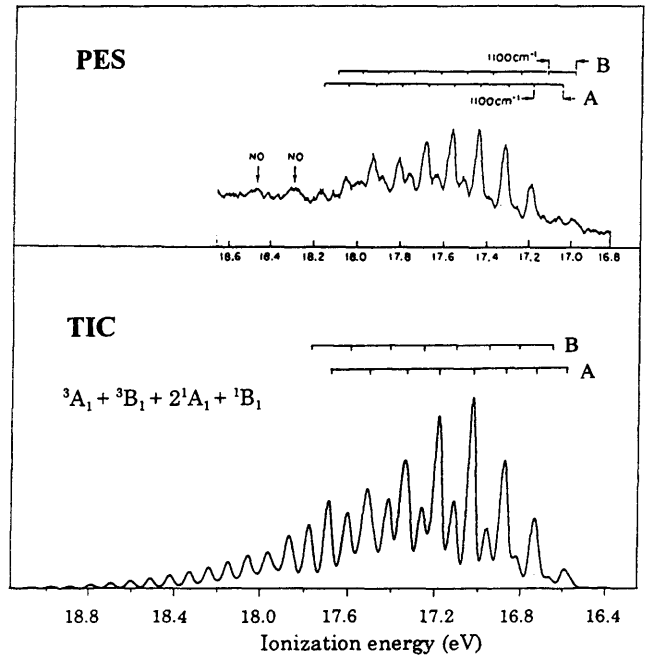

FIG. 6. The overall feature of the theoretical intensity curve of ionization of the $^1B_1$, $^3A_1$, $2\,^1A_1$, and $^3B_1$ states with a half width of 0.04 eV and the observed photoelectron spectrum from Brundle *et al.* (Ref. 2).

electron ionization from the main configuration of the ground state. Figure 6 shows the vibrational structure of the TIC, where the two vibrational progressions A and B are found. The vibrational structures below 17.4 eV are mainly a mixture of those of the $^3B_1$ and $^3A_1$ states. A contribution of the vibrational structure of the $2\,^1A_1$ state to the TIC becomes large above 17.4 eV. A contribution of the $^1B_1$ state to the TIC is negligibly small. Two vibrational progressions A and B are also found in the PES. Progression A has strong intensity, while progression B has weak intensity. Progressions A and B in the PES may correspond to progressions A and B in the TIC, respectively. Progression A in the TIC is made from the vibrational progressions of the (n 0, n =1–7) transitions of the $^3B_1$ state and the (n 0, n=1–6) transitions of the $^3A_1$ state, where each peak of the two progressions overlaps each other. The progression B in the TIC is ascribed to the vibrational progression B of the $^3B_1$ and $^3A_1$ states, where the vibrational transitions of the (n 1, n<6) and (n 3, n<5) levels contribute to the intensity. Brundle *et al.* have reported that the vibrational spacing was 1100 cm^{-1}, which may be assigned to the ν_1 frequency. The calculated values of the ν_1 frequencies of the $^3B_1$ and $^3A_1$ states are 1240 and 1202 cm^{-1}, respectively.

IV. CONCLUSION

We have studied the molecular structures, the vibrational eigenfunctions, the Franck–Condon factors, and the approximate theoretical intensity curves of eight ionic states ($^1A_1$, $^3B_2$, $^3A_2$, $^1A_2$, $^1B_2$, $^1B_1$, $2\,^1A_1$, $^3B_1$, and $^3A_1$) of NO_2 by vibrational calculations using the global region of the potential energy surface at the MRSDCI level.

The molecular structure of the $^1A_1$ state is linear, while those of the other states are bend.

The theoretical intensity curve of the first ionic state ($^1A_1$) does not reproduce well the photoelectron spectrum. The vibrational spacing corresponding to the ν_2 (O–N–O bending) mode, however, agrees with that of the PES. The present calculation shows that the two vibrational progressions contribute to the spectrum. One is the progressions of the ($2\ n$, $n=13-19$), ($4\ n$, $n=10-18$), and ($6\ n$, $n=11-14$) transitions, another is the progression of the ($3\ n$, $n=11-19$) and ($5\ n$, $n=10-16$) transitions.

The vibrational structure of the theoretical intensity curve of the $^3B_2$, $^3A_2$, $^1A_2$, and $^1B_2$ states reproduce well those of the photoelectron spectrum.

The $^1B_1$, $2\ ^1A_1$, $^3B_1$, and $^3A_1$ states contribute to the photoelectron spectrum in the 16.8–18.2 eV energy range. The contribution of the $^1B_1$ state, however, is negligible because of small value of the transition moment. The $2\ ^1A_1$ state contributes to the higher energy side of this band. The two vibrational progressions of the $^3B_1$ and $^3A_1$ states contribute to the vibrational structure of the lower energy side. One is the progression of the ($n\ 0$, $n=0-7$) transitions, which has strong intensity. Another is the progression of the ($n\ 1$, $n<6$) and ($n\ 3$, $n<5$) transitions, which has weak intensity.

[1] C. R. Brundle, Chem. Phys. Lett. **5**, 410 (1970).
[2] C. R. Brundle, D. Neumann, W. C. Price, D. Evans, A. W. Potts, and D. G. Streets, J. Chem. Phys. **53**, 705 (1970).
[3] D. W. Turner, A. D. Baker, C. Baker, and C. R. Brundle, *Molecular Photoelectron Spectroscopy* (Wiley, London, 1970).
[4] K. Kimura, S. Katsumata, Y. Achiba, T. Yamazaki, and S. Iwata, *Handbook of HeI Photoelectron Spectra of Fundamental Organic Molecules* (Halsted, New York, 1981).
[5] A. J. McKellar, D. Heryadi, D. L. Yeager, and J. A. Nichols, Chem. Phys. **238**, 1 (1998).
[6] H. Tatewaki and S. Huzinaga, J. Comput. Chem. **1**, 205 (1980).
[7] K. Takeshita and N. Shida, Chem. Phys. **210**, 461 (1996).
[8] B. H. Lengsfield III, J. Chem. Phys. **73**, 382 (1980).
[9] B. Liu and M. Yosimine, J. Chem. Phys. **74**, 612 (1981).
[10] B. H. Lengsfield III and B. Liu, J. Chem. Phys. **75**, 478 (1981).
[11] N. Shida, K. Takeshita, and Y. Yamamoto, Library program at the Hokkaido University Computing Center, 1993 (in Japanese).
[12] G. Herzberg, *Molecular Spectra and Molecular Structure, Part III* (van Nostrand, New York, 1966).